



Published in final edited form as:

Proc Am Control Conf. 2021 May ; 2021: . doi:10.23919/acc50511.2021.9482619.

Tracking Multiple Diffusing Particles Using Information Optimal Control

Samuel C. Pinto^{#1}, Nicholas A. Vickers^{#1}, Fatemeh Sharifi¹, Sean B. Andersson^{1,2}

¹Mechanical Engineering, Boston University, Boston, MA 02215, USA

²Division of Systems Engineering, Boston University, Boston, MA 02215, USA

These authors contributed equally to this work.

Abstract

We study the problem of tracking multiple diffusing particles using a laser scanning fluorescence microscope. The goal is to design trajectories for the laser to maximize the information contained in the measured intensity signal about the particles' trajectories. Our approach consists of a two level scheme: in the lower level we use an extremum seeking controller to track a single particle by first seeking it then orbiting around it. In the higher level controller, we decide which particle should be observed at each instant, with the goal of efficiently estimating each particle position while not losing track of any of them. Using simulations, we show that this technique is able to collect photons efficiently and to track multiple particles with low position estimation error.

I. Introduction

In the study of cellular biological systems, it is necessary to track and identify components of the cell such as enzymes, RNA, molecular machinery, and viral pathogens. One generically refers to these as “particles”. One set of methods for studying biology at these length scales are a group of techniques collectively referred to as single particle tracking (SPT) [1], [2]. In these methods, particles of interest are smaller than the diffraction limit of light but can be visualized by labeling them with a fluorescent tag, making them visible to a fluorescence microscope [3]. By tracking a particle over time, one can understand the particle's motion model and the value of its motion parameters. Additionally one can directly observe the particle's behavior and interactions within the cellular environment.

The application of SPT to the study of cellular biology has led to many breakthroughs in our understanding of subcellular processes. A few specific examples include measuring the behavior and roles of molecular motors [4], observing protein complex behavior in membrane localized processes [5], and discovering viral infection pathways [6]. In each of these cases, the transport of the target particles can only be interpreted with reference to the cellular context. In many cases, this context includes observing the transport of multiple particles simultaneously.

Tracking multiple particles in a fluorescence microscope can be achieved in a variety of ways. One common method is to acquire images with a laser scanning microscope, such as a confocal fluorescence microscope or two-photon fluorescence microscope. These

microscopes work by scanning a laser through a raster pattern to create an image. Unfortunately, the time to acquire a single image grows with the number of pixels in the image, making large area or high resolution images too slow for imaging dynamic particles. A paradigm change happened when feedback began to be used to control the laser position to track a single particle continuously without spending time away from the particle [7]. Previous work by one of the authors implemented this concept using an extremum seeking feedback formulation [8]. While there are benefits in terms of speed and resolution, the main limitation of feedback methods is that only one particle at a time can be tracked.

The need to track multiple particles motivated the development of more efficient (non-raster scanned) multiple particle tracking (MPT) methods. Earlier work extended the single particle feedback methods by tracking each particle individually and switching between particles at a constant rate [9], [10]. However, issues still remain such as the lack of a process to design efficient switching rules, the inability to simultaneously handle particles with different diffusion coefficients, and the challenge of collecting intensity signals that optimize the collected information in order to improve the particle position estimation performance. The contribution of this paper is to demonstrate a multiple particle tracking method that addresses these issues by combining a feedback driven tracking method with ideas from persistent monitoring (PM) of multiple uncertain targets. The feedback scheme is drawn from the extremum seeking (ES) approach, introduced in [11], where the trajectory of the laser is adapted based on the detected fluorescence. We contribute to this algorithm by showing that there is a set of parameters for which this tracking algorithm is maximally informative, i.e., we show that the laser converges to an orbital behavior where the collected data can be used to estimate the particle positions with minimal mean uncertainty. The system autonomously decides which particle should be tracked at each instant, using algorithms originally developed by our group in the context of PM [12]. In PM, the goal is to plan the trajectory of an autonomous agent that has to visit a set of targets in order to collect data that minimizes the targets states' estimation error. We integrate PM to the context of multiple particle tracking, where the SPT algorithm plays the role of "data collection" and PM is responsible for deciding the optimal time to switch from tracking one particle to another. After describing the approach, we demonstrate its effectiveness through simulations.

II. Problem Statement

In this section, we formally define the problem of tracking multiple particles with a laser scanning microscope. The goal of tracking these particles is to estimate their positions over time in the cellular context so that one can identify their motion model, as well as the values of the parameters that define the motion model accurately and precisely. For simplicity of exposition, we assume the dynamics of the particles of interest are given by a Brownian motion process, described in discrete time as

$$X_i[k] = X_i[k - 1] + W_i[k], \quad W_i[t] \sim \mathcal{N}(0, Q_i). \quad (1)$$

In this equation, X_i is a random variable taking values in \mathbb{R}^2 which represents the x and y location of particle i , where $i = 1, \dots, N$, and N is the number of tracked particles. $W_i[k]$ is a zero mean white noise with covariance matrix $Q_i = \text{diag}(2D_iT, 2D_iT)$, where D_i is the i -th particle diffusion coefficient, and T is the sampling period.

Photon detection is a Poisson random process called shot noise. The mean detected photon rate, I_i , for the fluorescent signal of a single particle at X_i and excited by a tightly focused laser beam centered at X_i is given by:

$$I_i = I_{0,i} \exp\left(-2 \frac{\|X_i - X_l\|^2}{b^2}\right), \quad (2)$$

where b is the laser beam width and $I_{0,i}$ is particle i 's peak mean detected photon rate, i.e. it is the mean intensity when the laser is positioned exactly above particle i . Given a sampling period T , the total mean detected intensity I for an integration time is the sum of each particle's contribution, given by

$$I = \sum_{i=1}^N I_i T. \quad (3)$$

We can directly control the laser position velocity (i.e., \dot{X}_l is the control input), and the laser maximum velocity is upper bounded by v_{\max} . Our goal is to control the laser position X_l such that the detected intensity signals can be used to efficiently estimate the particle trajectories. In other words, we want to define an online control strategy where the laser position is updated using some feedback law that aims to minimize the estimation error given by

$$\sum_{i=1}^N \sum_{k=1}^{N_s} E[\|\hat{X}_i[k] - X_i[k]\|^2], \quad (4)$$

where N_s is the total number of samples collected, and \hat{X}_i is estimated position of particle i generated using an offline estimator. Note that even though we use feedback while capturing the intensity data, the estimates of the particle positions are not necessarily computed simultaneously with the data acquisition process. Estimation can then be done offline. As a result there are no strict computational time constraints and the estimation can benefit from the entire dataset (as opposed to online methods, where the estimator must be causal). While the goal of this paper is the efficient *acquisition* of informative measurements, we do apply an offline estimator in our simulation results in Sec. V to help illustrate the results. However, a detailed study of estimator design is out of the scope of this paper. Interested readers should see e.g. [11], [13].

A. Proposed Solution

Our approach to this problem is to implement a two level control scheme. This allows us to divide the problem into two distinct parts, *measurement and tracking* of single particles (low level control), and *planning* which particle to measure and the duration of the measurement (high level control). One key assumption that enables this scheme is that the particles are separated enough so that detected photons comes from a single particle chosen by the high level controller. This assumption, while not always true in practice, is a common one in SPT and it allows us to approach the multiple particle tracking problem as being constituted of tracking individual particles sequentially and then cycling the laser between them. Extensions to denser collections of particles is left to future work. The low level control will be discussed in Sec. III and the higher level one in Sec. IV. Algorithm 1 describes precisely how the integration between the two controllers is to be done.

In Alg. 1, \hat{X}_i^{on} is an online estimate of the position of particle i , which means we need an online estimator for the interface between the lower level and the higher level controllers. We highlight that this online estimate needs to be computationally cheap and causal, and is usually not the same estimate that will be used offline (i.e. after all the data has been collected) to estimate the particle position with a high accuracy. In Alg. 1 the procedure `ScheduleNextObservedTarget(·, ·)` is what we call the “high level algorithm”.

Algorithm 1 Multiple Particle Tracking

```

1: while Experiment is Running do
2:    $[\tau, j] \leftarrow \text{ScheduleNextObservedTarget}(\hat{X}_i^{on}, i)$ 
3:   Move laser to  $\hat{X}_j$ .
4:   Run lower level control for  $\tau$  seconds.
5:   Update  $\hat{X}_j^{on}$ .
6:    $i \leftarrow j$ .

```

III. Extremum Seeking Single Particle Tracking

In this section, we discuss the lower level controller, responsible for tracking a single particle for some duration. Considering the goal of minimizing the estimation error in (4), one would like to design this controller such that the laser collects a photon signal that is maximally sensitive to small changes in particle position. In this context, we first analyze where is the best region to place the laser. We consider the random observation model with mean given by (2), and from it derive the Fisher Information Matrix (FIM) for estimating the particle position under the assumption of a fixed particle position. The FIM for a Poisson temporal random process is

$$\text{FIM}(X_i - X_l) = \int_{t_0}^{t_1} \frac{1}{I_i(X_i - X_l)} \frac{\partial I_i(X_i - X_l)}{\partial X_l} \frac{\partial I_i(X_i - X_l)^T}{\partial X_l} dt, \quad (5)$$

where the expected intensity I_i is given by (2) and $[t_0, t_1]$ is the time interval when particle i is being tracked [14]. We next apply the T-Optimality criteria to the FIM [15] to get the cost function

$$\begin{aligned}
J(X_i - X_l) &= \text{tr}(\text{FIM}(X_i - X_l)) \\
&= -\frac{16}{b^4} \int_{t_0}^{t_1} \|X_i - X_l\|^2 I_i(X_i - X_l) dt.
\end{aligned} \tag{6}$$

Optimizing (6) gives that the laser positions that minimize the trace of the FIM are given by a circle centered on the particle position with a radius of $\frac{b}{\sqrt{2}}$ [16]. We denote this set of positions as the information optimal orbit. In practice, the assumption we made about the particle position being fixed is not true. However, this information optimal orbit provides a near optimal result as long as the speed of the laser is fast relative to the particle motion.

The next step is to determine how to move the laser to the information optimal orbit when the particle position is not known exactly. The search for a practical controller to track a single particle leads us to select an extremum seeking controller (ESC). Extremum seeking is a model free method that locally explores a scalar field and drives the system state towards an extremal point in the field. In the case of SPT, the scalar field is the expected amount of detected photons which has a maximum centered on the particle's location. The use of ESC allows for tracking using only the collected intensity data, without the need of an online estimation scheme. (Note that our complete tracking scheme described in Subsec. II-A only needs an online estimate for the high level controller and, as will be discussed in Sec. IV, ESC can be used to provide this estimate.) A particular implementation of ESC that converges to an orbit around a field extremum and that has been shown to work well in SPT applications is that of a non-holonomic, reactive ESC [8], [17], [18] given by

$$\begin{aligned}
\Delta I &= I[k] - I[k-1], \\
\theta[k] &= \theta_0 + 2\pi f T - \frac{K_p}{T} \Delta I, \\
x_l[k] &= x_l[k-1] + 2\pi R f T \cos\theta[k-1], \\
y_l[k] &= y_l[k-1] + 2\pi R f T \sin\theta[k-1].
\end{aligned} \tag{7}$$

In these equations, f is its oscillation frequency, $\omega = 2\pi f$ is its angular frequency, T is the controller time step, and R is a positive constant. When $I = 0$, this controller imposes a circular orbit with radius R . The feedback term is responsible for guiding the system to an orbit centered at the extremum and radius R [18]. Therefore, when we set $R = b/\sqrt{2}$, ESC gives us a practical method for converging to the information optimal orbit and enables us to adapt the orbit as the particle moves.

We characterized the behavior of this lower level controller empirically. Fig. 1 shows the behavior of the ESC from two initial conditions with the particle being tracked at the origin. If the initial conditions are too far away, the photon rate is not high enough to drive the ESC to the target on any practical timescale. If the initial conditions are close enough, the ESC

converges to a cycle around the target. Empirically, we found there was a region of convergence defined by a circle with a radius approximately given by

$$r_c = b\sqrt{\frac{\ln(I_{0,i}T)}{2}} + R. \quad (8)$$

To illustrate the behavior of the convergence rate, we picked $K_p = 0.6$ and $\omega = 60$ Hz and plotted the number of cycles until convergence as a function of the starting position within the trackable region. The results are shown in Fig. 2.

The ESC is defined by three parameters, ω , K_p , and R . The radius is determined by the information optimal orbit while the other two can be tuned to minimize the tracking error. Using Monte Carlo simulations (that consider shot noise and used a diffusion coefficient of $D = 0.1$), we picked $f = 60$ Hz. The mean squared tracking error as a function of K_p is given in Fig. 3.

IV. Scheduling Multiple Particle Tracking

With the low level controller of Sec. III in place, in this section we turn to the specifics of our high level algorithm. In previous work by two of the authors [12], we explored the problem of persistent monitoring of a collection of targets using a (smaller) collection of agents. In this problem, an agent (the laser in the MPT setting) has to track the state (position) of a set of targets (the particles). This state was assumed to evolve with linear, time invariant stochastic dynamics (e.g. Brownian motion, given by a continuous time version of the dynamical model in (1)). Moreover, it was also assumed that when the agent dwelled at a target, the target state could be observed with the linear, stochastic observation model given by

$$Z(t) = C_i X_i(t) + V_i(t), \quad V_i(t) \sim \mathcal{N}(0, \mathcal{R}_i), \quad (9)$$

where X_i is the target state, \mathcal{R}_i is the covariance matrix of the observation and $V_i(t)$ is white noise process (i.e. $V_i(t_1)$ and $V_i(t_2)$ are uncorrelated if $t_1 \neq t_2$).

The goal of PM is to find the sequence of targets to be tracked and the dwelling time at each of them in order to minimize the worst-case estimation error over long time horizons, i.e.

$$\min_{\mathcal{T}} \max_{\forall 1 \leq i \leq N} \limsup_{t \rightarrow \infty} \text{tr}(\Omega_i(t)), \quad (10)$$

where $\Omega_i(t)$ is the covariance matrix of an online estimator $\hat{X}_i^{on}(t)$ of the state $X_i(t)$, \mathcal{T} is the vector that contains the time spent tracking each particle, and \mathcal{V} is the sequence of particles visited.

For this cost function (10), for any given dwelling times \mathcal{T} , the optimal visiting sequence is given by the solution of the Traveling Salesman Problem (TSP) [12], [19], which consists of finding the shortest path that is able to track all the particles. While the TSP is NP-hard and

finding an exact solution is infeasible for a large number of targets, there are well-known efficient sub-optimal solutions that can be applied in practice. Then, given a visiting sequence, the optimal visiting times can be calculated using a consensus-type algorithm; see [12] for details.

To deploy the PM algorithm, we need a simple online estimate that fits our estimation model (9). This is provided by ESC since, after convergence to the radius R , it produces unbiased observations Z according to the following relation:

$$Z = X_i + \begin{bmatrix} -R \sin \theta \\ R \cos \theta \end{bmatrix} = X_i + \tilde{V}_i, \quad (11)$$

where \tilde{V}_i is a noise term.

With this estimator, the PM algorithm determines the sequence for visiting the particles and the time to spend at each particle. Intuitively, PM seeks to balance the time spent at each of the particles, trading off estimation accuracy at any given particle for performance over the entire collection of particles.

In the MPT setting, when the laser transitions to visit a given particle, it moves to the particle's last estimated position (as indicated in Alg. 1), as this is the most likely particle position and the expected intensity signal is higher when the particle is closer to the laser. The cost function (10) aims to minimize the worst case uncertainty on the particles' estimated position and this maximizes the chances that the observations acquire enough photons for ESC to converge to an orbit centered in the particle.

Finally, we note that in the original PM formulation in [12], the targets (particles) were assumed to be fixed. Here we rely on the assumption that their movement is slow compared to the laser speed and thus the PM algorithm produces near optimal schedules.

V. Simulation and Results

In this section, we provide a set of simulations (with three particles in each) with the goal of illustrating the performance of our proposed approach for tracking multiple particles. For these simulations, we used the Brownian motion model in (1) and the laser observation model in (2), with the parameters: $D_i = 0.1 \mu\text{m}^2/\text{s}$, $I_{0,i} = 5 \times 10^4$ photons/s, $b = 0.5 \mu\text{m}$. The maximum laser speed was limited to $v_{\max} = 300 \mu\text{m}/\text{s}$ and the simulation time-step was set to $T = 10^{-4}$ s. The extremum seeking oscillation frequency was set to $f = 60$ Hz, its gain to $k_p = 0.2$ and the radius to $R = b/\sqrt{2}$. The value of the covariance of the noise \tilde{V}_i in the observation model was obtained using the simulated mean squared tracking error, given in Fig. 3. The particles' initial positions were drawn from a uniform distribution in $[0 \mu\text{m}, 10 \mu\text{m}] \times [0 \mu\text{m}, 10 \mu\text{m}]$. In the initialization, we assumed that the controller had access to the approximate initial position of the particles plus some zero mean Gaussian noise (with covariance equals to $\text{diag}(0.02^2, 0.02^2)$) μm^2 . In practical settings, this initial position could be obtained using, for example, a widefield image. The initial position of the laser was $[5 \mu\text{m}, 5 \mu\text{m}]$ and the total simulation time was 1 s.

To characterize the performance of the tracking algorithm, we analyzed the rate of collected photons. Note that although the number of collected photons does not directly translate into estimation performance (in particular the position where the photons were collected is also important), it is still a good proxy for evaluating tracking performance, since in general, increasing the number of collected photons increases the estimation performance.

The trajectory and the collected photons per sample for typical run of the simulation are shown in Figs. 4 and 5, respectively. The colors in the intensity figure match the particle from which those photons came from. Note that since the particles were widely spaced, all photons collected at each time step were from a single particle. In this run, the mean collected photons rate (normalized by I_0) was 0.2905/sec. This typical run is also displayed in a video available in the link [20].

To get a sense of the average performance of the tracking scheme, we ran 100 simulations with the same parameters, but with different initial positions and Brownian motion realizations. The average detected photons rate over these runs was $0.2958 \times I_0$.

While the ESC does not use any model information, the high-level PM planner uses prior knowledge of the process and observation noises. In practice, of course, these terms are at best known only approximately. In order to illustrate the performance of our tracking scheme to perturbations in the system parameters, we ran set of simulation with almost the same setup as in the previously described scenarios, except that the values of the peak intensity and diffusion coefficient were modified to $I_0 = 4 \times 10^4$ photons/s and $D = 0.11 \mu\text{m}^2/\text{s}$. The controller was the same as with the nominal parameters. In these simulations, the average detected photons rate per second was $0.2703 \times I_0$.

Finally, in order to give a sense of how our approach compares to a simple raster scan, we also used the intensity signal for a raster scan trajectory. In this setup, the laser moved along a zig-zag (raster) pattern with constant speed, equal to v_{\max} . The raster scan trajectory is shown in Fig. 6. Note that while the raster scan images a large region without any particles, this is normal to raster scanning as the region is set in open loop fashion. This simulation run yielded a normalized average photon rate of 0.0132.

Table I summarizes the results simulation using the setups above mentioned. Each setup was run 100 times, with random initial positions and diffusion noise realizations. The rate of acquired photons was consistent among the different simulation runs using our tracking method and much higher than when using a raster scan.

A. Trajectory estimation from photon data

Although this paper focuses on data collection, the overall goal of MPT is to accurately estimate the particles' positions *offline*. To illustrate how this can be done using the intensity data from our simulations, we estimated the particles' positions by applying a Particle Filter and Rauch-Tung-Striebel Smoother (see e.g. [13]). We note that we have not extensively explored different offline estimators and likely other approaches could yield estimation with lower errors. The mean estimation error over time in the first scenario is shown in Fig. 7. The RMSE was calculated using

$$RMSE = \|(\hat{X}_i - X_i)\|. \quad (12)$$

RMSE results for the third simulation setting (with perturbed parameters) is shown in Fig. 8. In these plots, the shaded regions indicate times when an individual particle is being tracked. The RMSE of all runs and considering all simulation setups is given in Table II. Our estimation algorithm was able to keep the average error at around 100 nm when the nominal parameters were used in this simulation. However, the mismatch in $D_i I_{0,i}$, generated a higher estimation error. In future work we plan to also estimate the model parameters along with the particles' positions, aiming to improve our estimation performance and robustness to modeling imperfections.

VI. Conclusions and Future Work

In this paper, we proposed an approach to control the laser position of a laser scanning microscope in order to generate intensity data that can be efficiently used to track multiple particles in a sample. Our algorithm consisted of two controllers, one responsible for locally tracking a single particle and another one that plans which particle to be tracked at each instant. Simulation results showed that our algorithm was able to efficiently track each of the particles and acquire a large number of photons and initial results indicate much better performance than a simple raster scan.

In future works, we plan to drop the assumption that the particle diffusion parameters and the peak intensity are known beforehand, estimate them while we run our control algorithm, and then refine this estimate offline using, for example, Expectation Maximization to jointly optimize the particle position and model parameter estimates. Additionally, we plan to run physical experiments to validate our approach in a real world scenario.

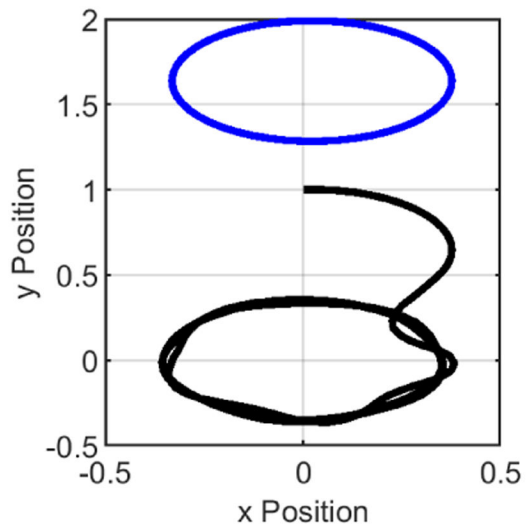
Acknowledgement

This work was supported in part by NSF through ECCS-1931600 and by NIH through 1R01GM117039-01A1.

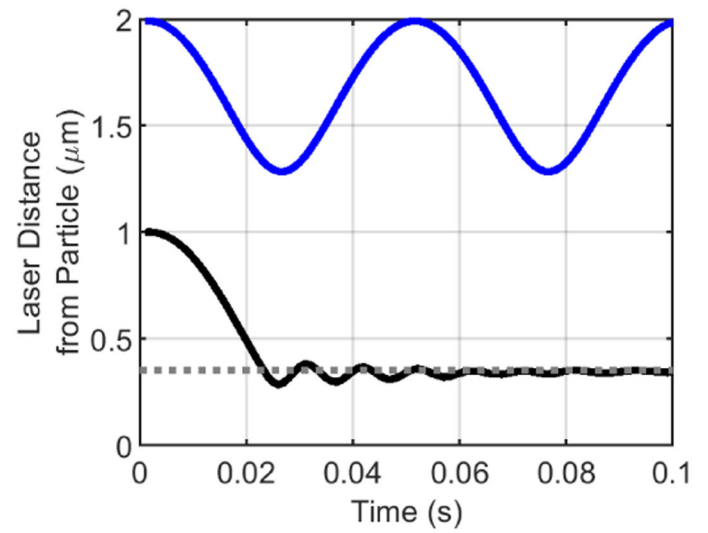
References

- [1]. Manzo C and Garcia-Parajo MF, "A review of progress in single particle tracking: from methods to biophysical insights," Reports on Progress in Physics, vol. 78, no. 12, p. 124601, 2015. [PubMed: 26511974]
- [2]. Shen H, Tauzin LJ, Baiyasi R, Wang W, Moringo N, Shuang B, and Landes CF, "Single particle tracking: from theory to biophysical applications," Chemical reviews, vol. 117, no. 11, pp. 7331–7376, 2017. [PubMed: 28520419]
- [3]. Mondal PP and Diaspro A, Fundamentals of fluorescence microscopy: exploring life with light. Springer Science & Business Media, 2013.
- [4]. Kural C, Balci H, and Selvin PR, "Molecular motors one at a time: Fiona to the rescue," Journal of Physics: Condensed Matter, vol. 17, no. 47, p. S3979, 2005. [PubMed: 21690736]
- [5]. Aguet F, Upadhyayula S, Gaudin R, Chou Y.-y., Cocucci E, He K, Chen B-C, Mosaliganti K, Pasham M, Skillern Wet al., "Membrane dynamics of dividing cells imaged by lattice light-sheet microscopy," Molecular Biology of the Cell, vol. 27, no. 22, pp. 3418–3435, 2016. [PubMed: 27535432]

- [6]. Brandenburg B and Zhuang X, "Virus trafficking—learning from single-virus tracking," *Nature Reviews Microbiology*, vol. 5, no. 3, p. 197, 2007. [PubMed: 17304249]
- [7]. Enderlein J, "Tracking of fluorescent molecules diffusing within membranes," *Applied Physics B*, vol. 71, no. 5, pp. 773–777, 2000.
- [8]. Andersson SB, "A nonlinear controller for three-dimensional tracking of a fluorescent particle in a confocal microscope," *Applied Physics B*, vol. 104, no. 1, pp. 161–173, 2011.
- [9]. Shen Z and Andersson SB, "LQG-based tracking of multiple fluorescent particles in two-dimensions in a confocal microscope," in *2009 American Control Conference*, 2009, pp. 1682–1687.
- [10]. Shen Z and Andersson SB, "Tracking multiple fluorescent particles in two dimensions in a confocal microscope," in *Proceedings of the 48th IEEE Conference on Decision and Control (CDC) held jointly with 2009 28th Chinese Control Conference*. IEEE, 2009, pp. 6052–6057.
- [11]. Ashley TT, Gan EL, Pan J, and Andersson SB, "Tracking single fluorescent particles in three dimensions via extremum seeking," *Biomedical Optics Express*, vol. 7, no. 9, pp. 3355–3376, 2016. [PubMed: 27699104]
- [12]. Pinto SC, Andersson SB, Hendrickx JM, and Cassandras CG, "A minimax approach to sensor scheduling on graphs," in *American Control Conference*, 2021.
- [13]. Lin Y and Andersson SB, "Simultaneous localization and parameter estimation for single particle tracking via sigma points based EM," in *2019 IEEE 58th Conference on Decision and Control (CDC)*. IEEE, 2019, pp. 6467–6472.
- [14]. Snyder DL and Miller MI, *Random point processes in time and space*. Springer Science & Business Media, 2012.
- [15]. Pukelsheim F, *Optimal design of experiments*. SIAM, 2006.
- [16]. Gallatin GM and Berglund AJ, "Optimal laser scan path for localizing a fluorescent particle in two or three dimensions," *Optics Express*, vol. 20, no. 15, pp. 16 381–16 393, 2012.
- [17]. Ashley TT and Andersson SB, "A control law for seeking an extremum of a three-dimensional scalar potential field," in *2016 American Control Conference (ACC)*. IEEE, 2016, pp. 6103–6108.
- [18]. Ashley TT and Andersson SB, "Tracking a diffusing three-dimensional source via nonholonomic extremum seeking," *IEEE Transactions on Automatic Control*, vol. 63, no. 9, pp. 2855–2866, 2017.
- [19]. Applegate DL, Bixby RE, Chvatal V, and Cook WJ, *The traveling salesman problem: a computational study*. Princeton University Press, 2006.
- [20]. Pinto SC, Vickers NA, Sharifi F, and Andersson SB. Video of typical MPT simulation run. Youtube. [Online]. Available: <https://youtu.be/J4ZKafMMOs>



(a) Laser trajectory



(b) Laser distance from particle

Fig. 1. Extremum Seeking Controller trajectories starting at two different positions showing failure to converge (blue), and convergence (black).

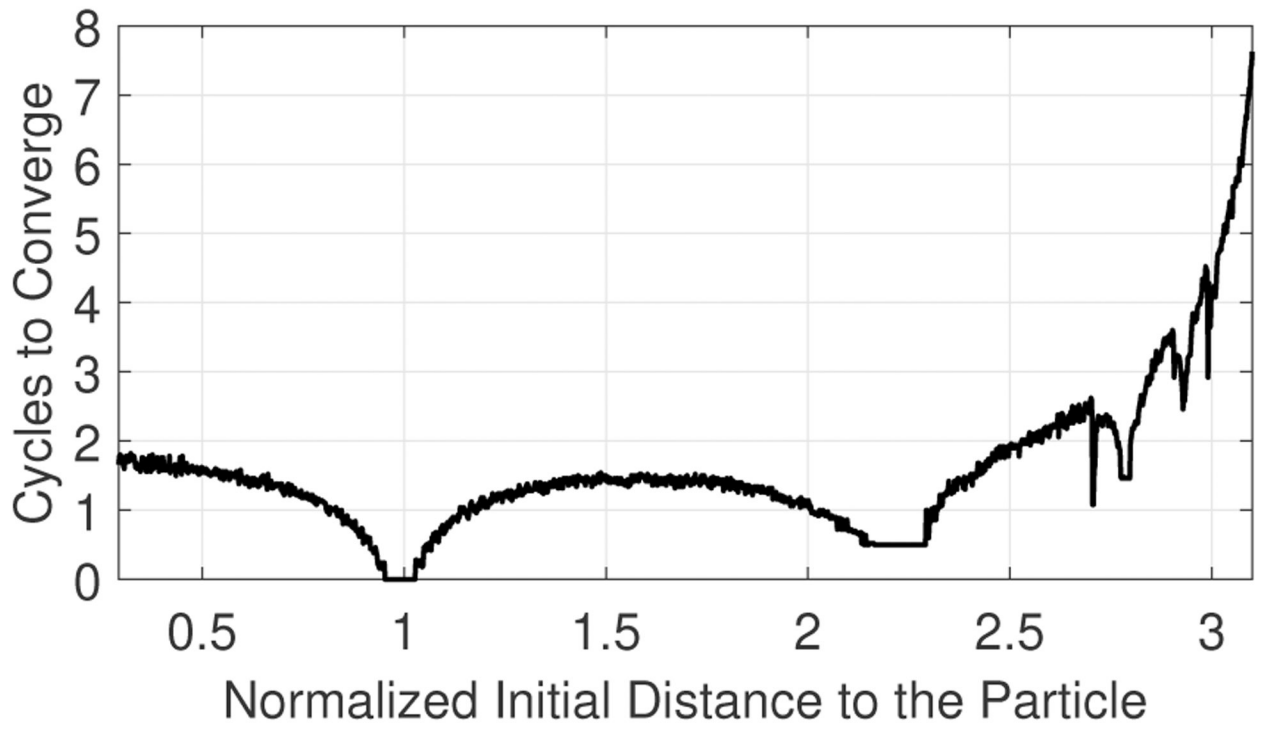


Fig. 2. Number of cycles to convergence as a function of the initial relative position of the laser and particle. The initial distance is normalized by the radius R .

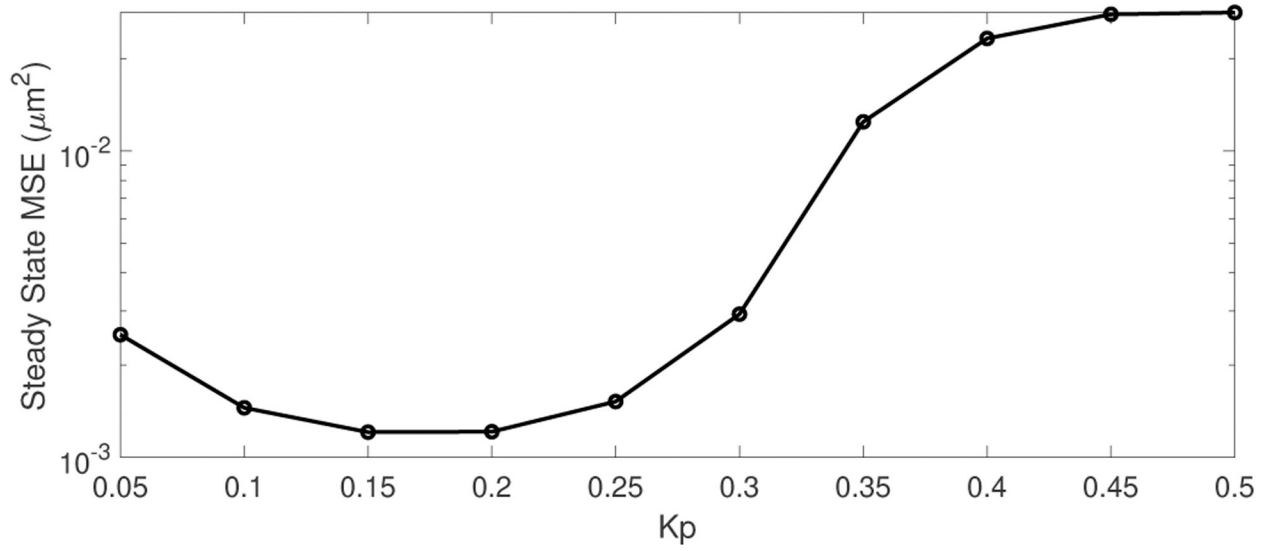


Fig. 3.

Mean squared tracking error as a function of K_p , for $f = 60$ Hz and particle diffusion coefficient $D_x = D_y = 0.1 \mu\text{m}^2/\text{s}$.

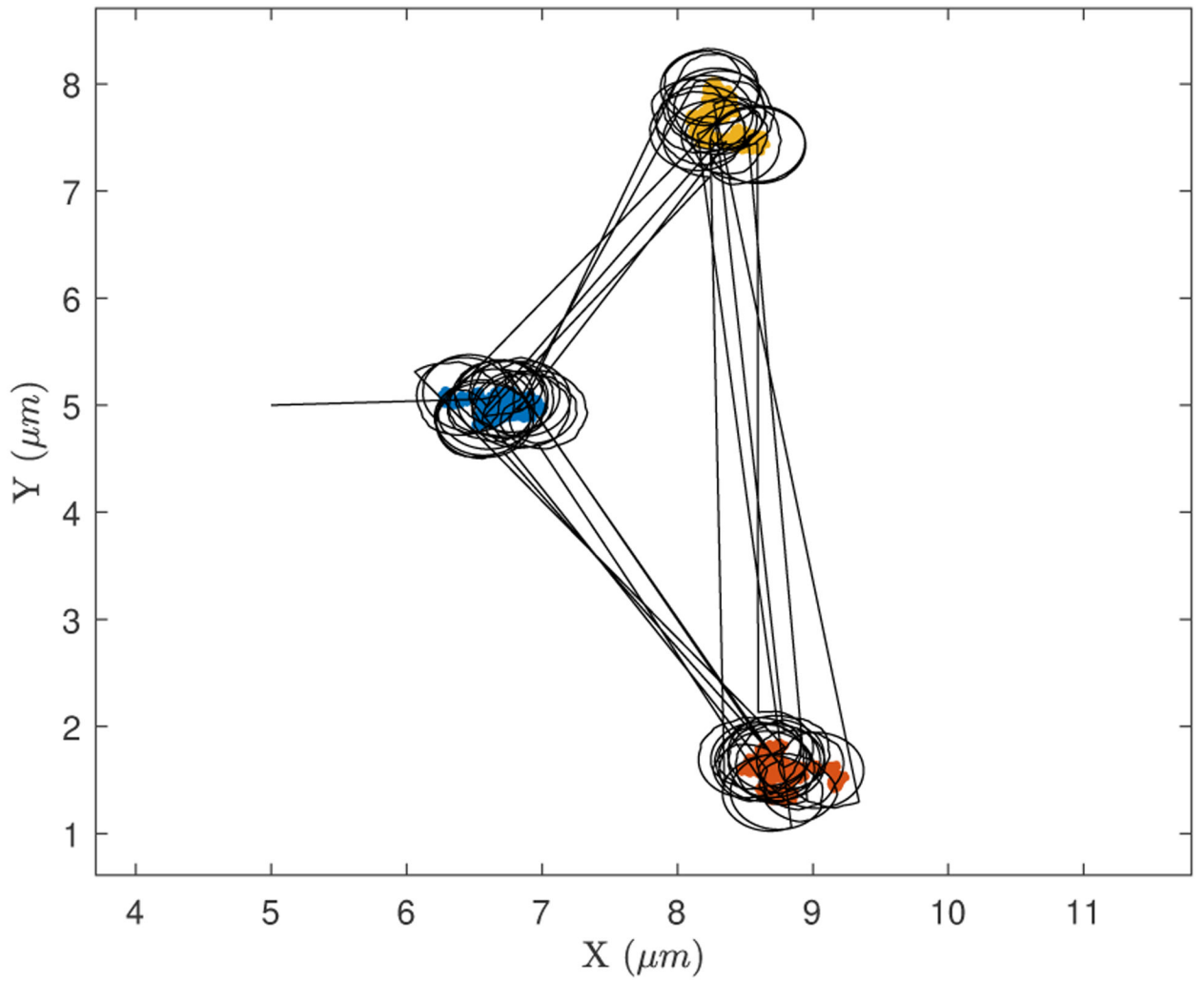


Fig. 4. Particle and laser trajectories, while tracking three particles in the first simulation scenario. The laser trajectory is in black and the particles are in blue, yellow and red.

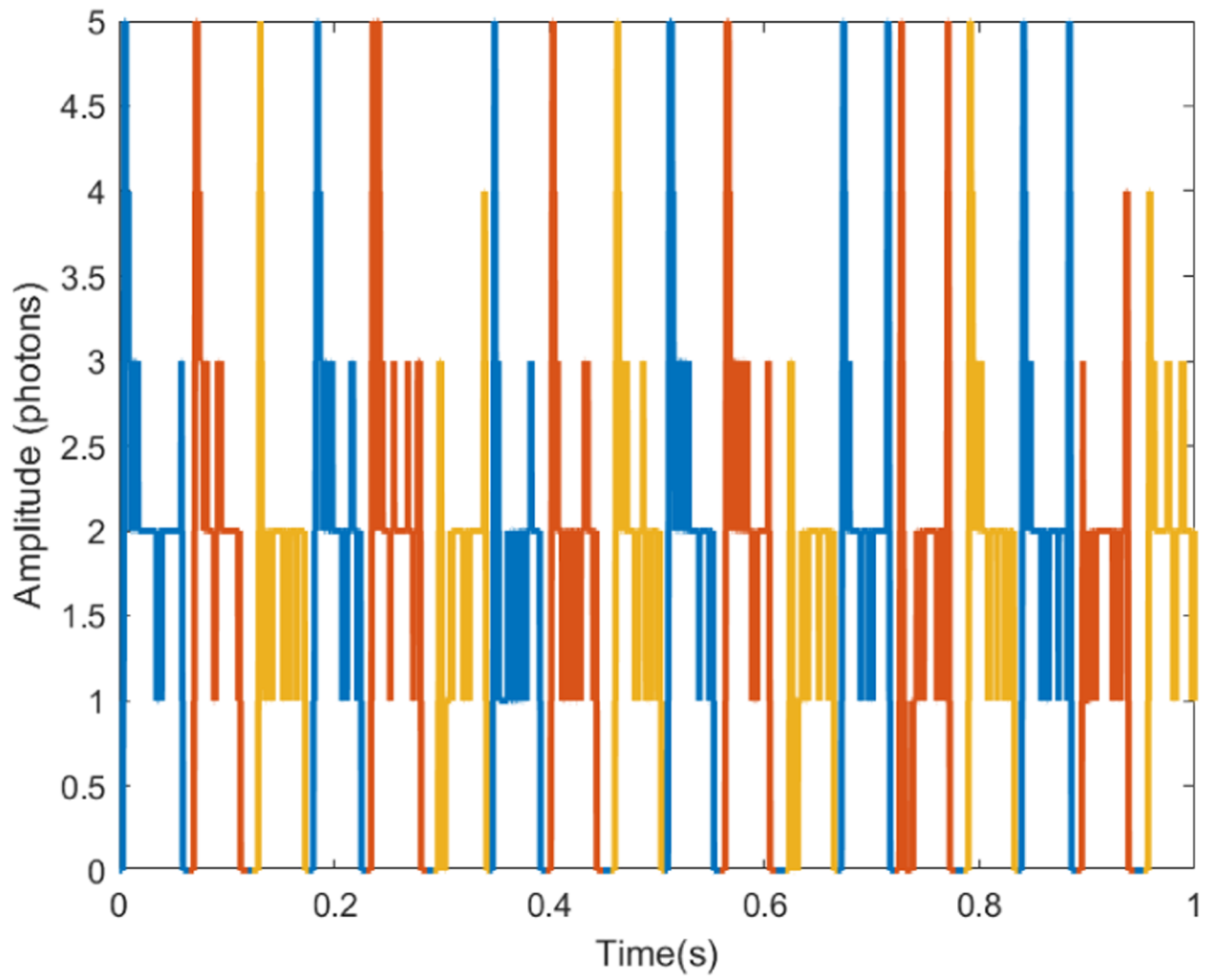


Fig. 5. Photons collected at each time step ($T = 10^{-4}$ s) in the first simulation scenario. The colors in the plot indicate which particle emitted those photon.

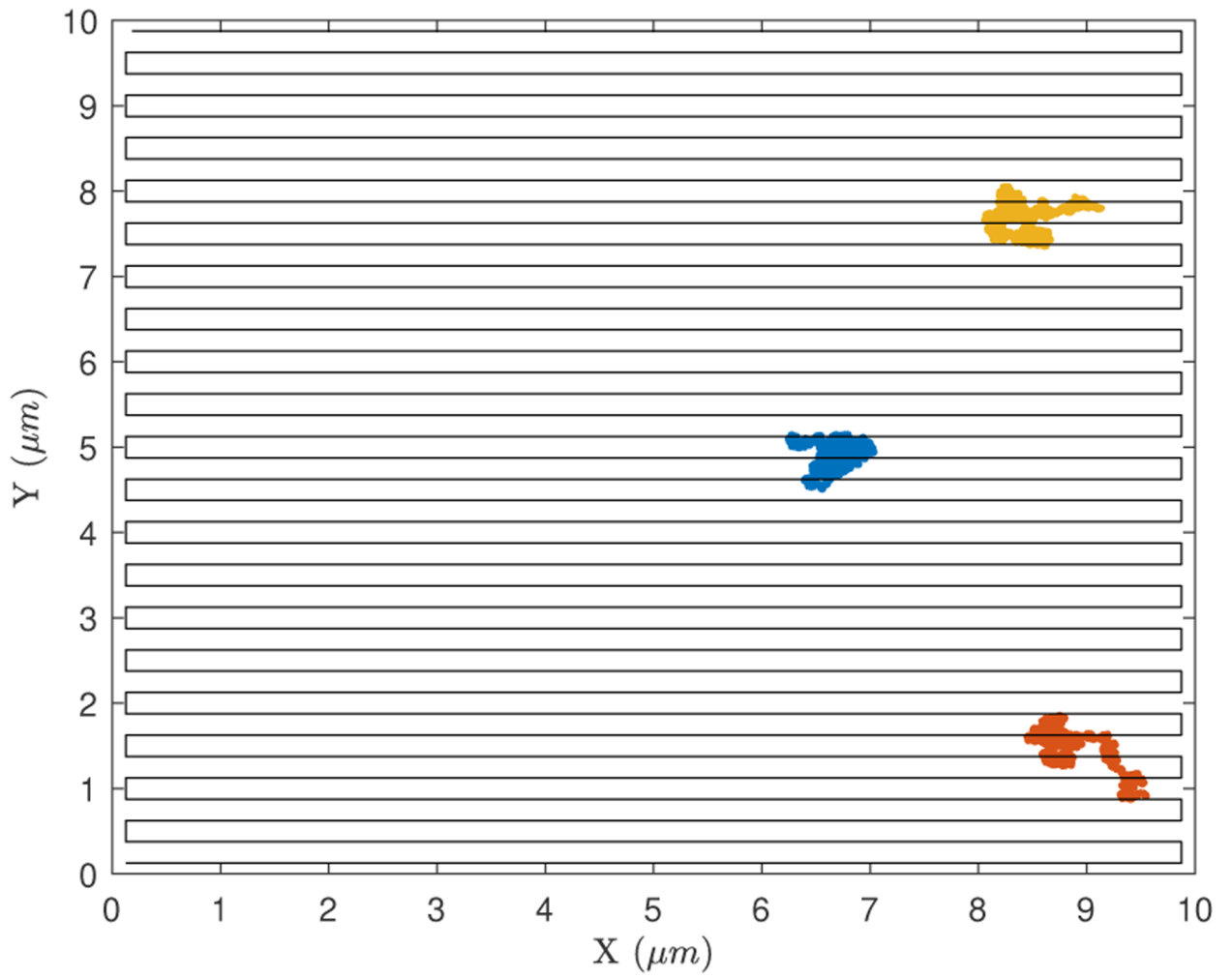


Fig. 6. Illustration of a raster scanning trajectory considering a similar simulation setup. The agent trajectory is in black, while the particle trajectories are colored.

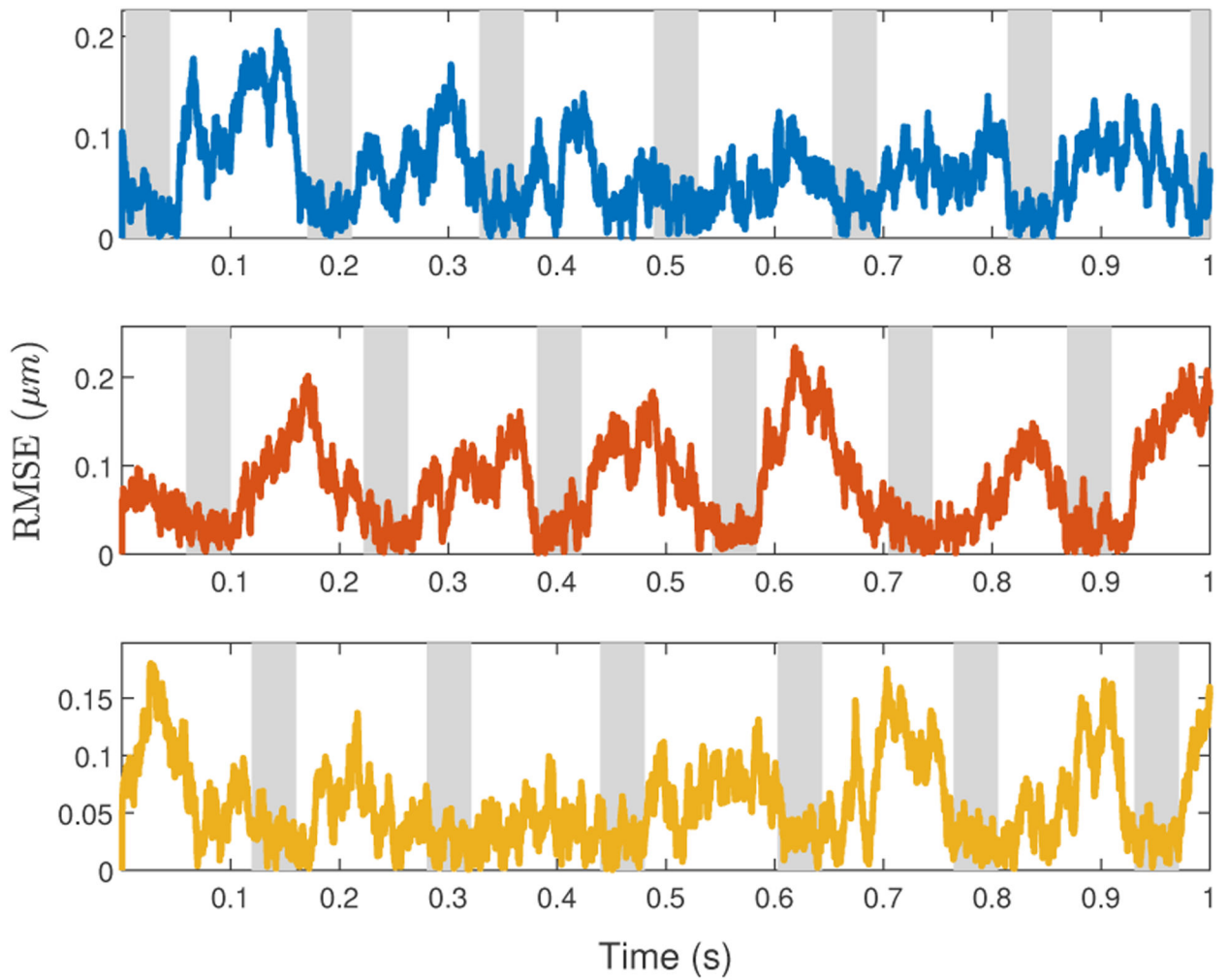


Fig. 7. Estimation error over time using the offline estimator. The colors of the plots match the colors of the particle in Fig. 4. The shaded areas mark when the laser was orbiting around each particle.

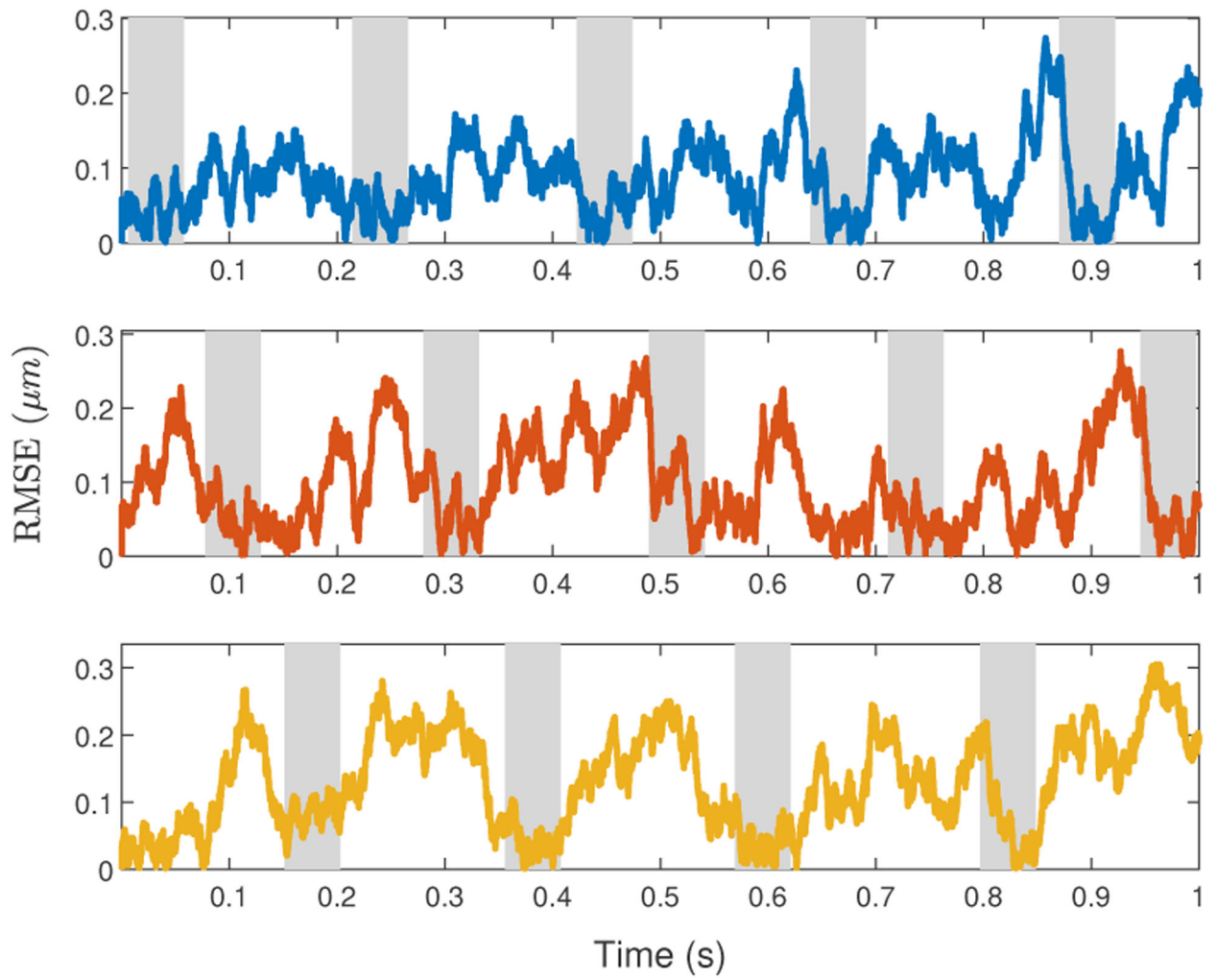


Fig. 8. Estimation error over time with perturbed parameters. The shaded areas mark when the laser was orbiting around each particle.

TABLE I

Mean number of collected photons per second normalized by $I_{0,i}$ for 100 runs of each of the simulation setups.

Nominal params.	Perturbed params	Raster scan
0.2958 ± 0.0235	0.2703 ± 0.0795	0.0111 ± 0.0033

Author Manuscript

Author Manuscript

Author Manuscript

Author Manuscript

TABLE II

RMSE Estimation error of 100 simulation runs.

Nominal params.	Perturbed params
100.3 ± 38.1 nm	138.4 ± 66.3 nm

Author Manuscript

Author Manuscript

Author Manuscript

Author Manuscript